

## Effects of Ta on the magnetic structure of permalloy

Nassrin Y. Moghadam,<sup>a)</sup> G. M. Stocks, M. Kowalewski, and W. H. Butler  
Oak Ridge National Laboratory, Oak Ridge, Tennessee 37831-6114

In permalloy (Py) based heterostructures Ta has deleterious effects on the magnetic properties resulting in magnetic dead layers. Using the Korringa–Kohn–Rostoker coherent potential approximation method, it is shown that the average moment of Py ( $\text{Ni}_{0.8}\text{Fe}_{0.2}$ ) is rapidly quenched by Ta substitutional additions. Locally self-consistent multiple-scattering method calculations for large supercell models of  $\text{Py}_{0.9}\text{Ta}_{0.1}$  show that Ta additions also result in substantial fluctuations in the size of the local moments. The configuration dependent reductions in the local moments are larger for Ni than for Fe sites and are the largest for Ni sites closest to Ta. © 2001 American Institute of Physics. [DOI: 10.1063/1.1356032]

### I. INTRODUCTION

Tantalum is widely used in magnetic random access memory (MRAM) devices. It is used to prevent damage to the semiconducting substrate during the patterning of the memory cells and also to promote the growth of the giant magnetoresistance (GMR) layers. GMR devices generally require two magnetic layers, typically thin layers of permalloy (a  $\text{Ni}_{0.8}\text{Fe}_{0.2}$  fcc solid solution) separated by a nonmagnetic spacer layer. It is known that Ta has deleterious effects on the magnetic properties. Experimental studies of the effects of Ta on the magnetic thickness of permalloy films show that tantalum is primarily responsible for the loss of moment in MRAM devices.<sup>1</sup> These experimental measurements show a loss of moment equivalent to a magnetic dead layer thickness of  $1.5 \pm 0.2$  nm for as-deposited films and  $1.7 \pm 0.2$  nm for the films annealed at 525 K.

Here we present first-principles studies of the effects of tantalum on the magnetic properties of permalloy (Py). Two methods are used, the Korringa–Kohn–Rostoker coherent potential approximation (KKR-CPA),<sup>2,3</sup> and the locally self-consistent multiple-scattering (LSMS)<sup>4,5</sup> method. The KKR-CPA is a first-principles method that treats the effects of disorder on the electronic structure. Experience has shown that the KKR-CPA gives a good account of configurationally averaged properties such as the configurationally averaged density of states  $\langle n(\epsilon) \rangle$  and magnetic moment  $\langle M \rangle$ . Using the LSMS method, disorder is treated by the use of large supercell models in which the atomic species are randomly distributed. Contrary to the KKR-CPA method, local fluctuation effects as well as full treatment of Coulomb energy are included. This article is arranged as follows. In Sec. II details of the KKR-CPA and the LSMS calculations are discussed. Numerical results are presented in Sec. III. A discussion of the results concludes the article.

### II. COMPUTATIONAL APPROACH

Permalloy and permalloy-Ta alloys are both modeled as fcc solid solutions. The lattice parameter is taken to be 6.705

Bohr. The atoms are assumed to occupy the ideal positions. Thus strain fluctuations are neglected even for additions of the much larger Ta atoms.

The KKR-CPA and LSMS methods are both based on Green's function approach to multiple-scattering theory (MST)<sup>6</sup> and use local spin density approximation to density functional theory (LDA-DFT).<sup>7,8</sup> In both methods we treat the core and semicore states relativistically and the valence states semirelativistically. The charge density is determined by integrating the Green's function along a semicircular contour in the upper half of the complex energy plane using 30 energy points. For density of states (DOS) calculations, an energy contour is taken that is parallel to the real axis with an imaginary part  $\text{Im } \epsilon \sim 0.001$  Ry. About 110 energies (real part of) are used to span the occupied bands.

In the KKR-CPA calculations, the equations are solved in  $\mathbf{k}$ -space and Brillouin zone integrations are performed using the prism method.<sup>9</sup> A maximum angular momentum cut-off of  $l_{\text{max}}=3$  and the muffin tin (MT) approximation to the potential are used. The configurationally averaged DOS  $\langle n(\epsilon) \rangle$  and magnetic moment  $\langle M \rangle$  are obtained from

$$\langle n(\epsilon) \rangle_{\text{alloy}} = \sum_{\alpha} c_{\alpha} \langle n(\epsilon) \rangle_{\alpha} \quad (1)$$

and

$$\langle M \rangle_{\text{alloy}} = \sum_{\alpha} c_{\alpha} \langle M \rangle_{\alpha}, \quad (2)$$

where  $c_{\alpha}$  is the concentration of the  $\alpha$ th species, and  $\langle n(\epsilon) \rangle_{\alpha}$  and  $\langle M \rangle_{\alpha}$  are the single-site averaged DOS and magnetic moments.

In the LSMS calculations, the alloy is modeled by a 108 atom supercell consisting of a  $3 \times 3 \times 3$  repeat of the underlying fcc lattice. This number of atoms is sufficient to make the calculated properties reasonably self-averaging. A random number generator is used to distribute the atomic species amongst the sites according to their concentration. The Wigner–Seitz volumes are constructed around each atom such that the atomic size mismatch between different species is taken into account. The cell potentials are taken to be of the ASA-MT form.<sup>10</sup> The ASA-MT is a spherical approximation to the potential that combines the strengths of both

<sup>a)</sup>Electronic mail: nassrin@gmsis.ms.ornl.gov

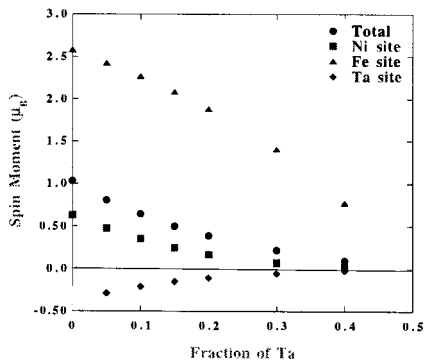


FIG. 1. Concentration dependence of the configurationally averaged total and component spin moments in permalloy-Ta alloys calculated using the KKR-CPA method.

MT and atomic sphere approximations (ASA), and at the same time, overcomes some of the limitations of these methods. In the LSMS method, the KKR matrix is calculated in real space with a local interaction zone (LIZ) that includes the central site and six near neighbor (nn) shells (87 atoms). The value of the  $l_{max}$  is chosen to be 8 on the central site, 3 on the first and the second nn shells and 2 on the remaining shells within LIZ. Test studies show that putting large  $l_{max}$  on shells beyond the first nn shell changes the energy by  $<0.02$  mRy.

In the LSMS method, configurationally averaged species dependent DOS and moments can be calculated from

$$\langle n(\epsilon) \rangle_\alpha = 1/N_\alpha \sum_{i=\alpha} n^i(\epsilon) \tag{3}$$

and

$$\langle M \rangle_\alpha = 1/N_\alpha \sum_{i=\alpha} m^i, \tag{4}$$

where  $n^i(\epsilon)$  and  $m^i$  are individual site DOS and moments in the supercell and  $N_\alpha$  is the number of sites occupied by the  $\alpha$  species.

### III. RESULTS

In Fig. 1 we show the results of KKR-CPA calculations of the concentration dependence of the configurationally averaged total and component spin moments of  $Py_{1-c}Ta_c$  alloys. The average moment is projected to vanish at a concentration of  $\sim 50\%$  Ta. Both Fe and Ni configurationally averaged site moments decrease rapidly upon the addition of Ta, and a small negative moment is induced at Ta sites.

Detailed analysis of the DOS shows that magnetism is Stoner-like. As an example of the effect of disorder on the electronic structure, in Fig. 2, we show the calculated DOS for  $Py_{0.9}Ta_{0.1}$ . As is the case for Py, the Ni and Fe majority  $d$ -scattering resonances are at essentially the same energy resulting in rigid band-like behavior and a sharp DOS damped only by the presence of Ta. For the minority states, even in Py there is considerable broadening of the DOS resulting from the large separation of Fe and Ni minority  $d$ -scattering resonances (by approximating the exchange splitting). This damping is further accentuated by Ta addi-

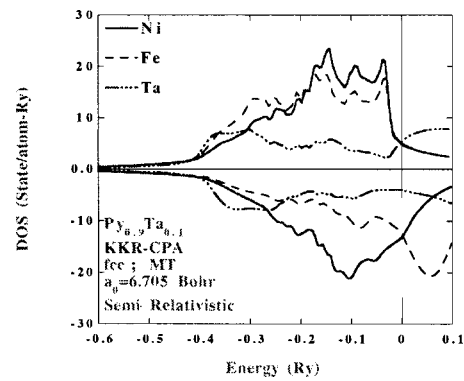


FIG. 2. DOS for  $Py_{0.9}Ta_{0.1}$  as a function of energy relative to Fermi energy (vertical line). Solid curve: average DOS on the Ni site; dashed curve: average DOS on the Fe site; and line-dash curve: average DOS on the Ta site. DOS for spin up electrons are plotted above and those for spin down electrons are plotted below the energy axis.

tions. The Ta states themselves are massively broadened by the effects of disorder due to a large separation between the Ta and Fe and Ni scattering resonances for both spin channels. For this concentration the reduction in the average moment is proportional to the reduction in the exchange splitting indicating Stoner behavior.

While the KKR-CPA method describes the configurationally averaged single-site properties, it does not yield any information about fluctuations in moments and electronic structure about the average that result from specific local atomic arrangements. These fluctuations are illustrated in Fig. 3 where we show the spin moments  $m^i$  for all sites in the 108 atom supercell model of  $Py_{0.9}Ta_{0.1}$  that are obtained using the LSMS method. The large positive moments correspond to Fe sites, the smaller positive moments to Ni sites, and the negative moments to Ta sites. Significant fluctuations and reductions of moments are observed at both Ni and Fe sites compared to the values in Py. Moreover, the reductions are larger on Ni atoms that are closer to Ta. The fluctuations and reductions are smaller at Fe sites. The large moment fluctuations are contrary to the behavior in Py, where the magnitudes of the moments on Ni and Fe sites show small fluctuations.

For the configurationally averaged spin moments we show in Table I a comparison between the values calculated

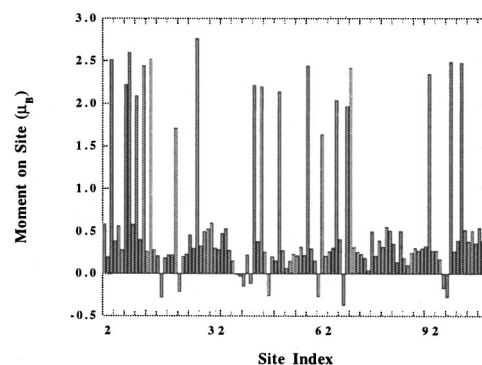


FIG. 3. Site specific spin moments in  $Py_{0.9}Ta_{0.1}$  calculated using the LSMS method for a supercell model consisting of 108 sites (78 Ni, 19 Fe, and 11 Ta atoms).

TABLE I. Calculated configurationally averaged total and component spin moments for Py and  $\text{Py}_{0.9}\text{Ta}_{0.1}$  using the KKR-CPA and the LSMS methods. The moments are in units of  $\mu_B$ .

	KKR-CPA		LSMS	
	Py	$\text{Py}_{0.9}\text{Ta}_{0.1}$	Py	$\text{Py}_{0.9}\text{Ta}_{0.1}$
$\langle M \rangle_{\text{alloy}}$	1.03	0.64	1.02	0.61
$\langle M \rangle_{\text{Ni}}$	0.63	0.36	0.60	0.31
$\langle M \rangle_{\text{Fe}}$	2.58	2.27	2.68	2.27
$\langle M \rangle_{\text{Ta}}$		-0.21		-0.20

using the LSMS and the KKR-CPA methods for the  $\text{Py}_{0.9}\text{Ta}_{0.1}$  alloy. Corresponding results for Py are listed for comparison. It is seen that the values obtained from the LSMS calculations are in good agreement with those obtained from the KKR-CPA method. Note that the KKR-CPA yields properties of the alloy that are averaged over all possible configurations. Therefore it is not surprising that once the site moments, as calculated by the LSMS, are averaged over, the results are similar to the KKR-CPA.

#### IV. CONCLUSIONS

Effects of Ta on the magnetic structure of permalloy are studied using the real space LSMS method and supercell models and the  $\mathbf{k}$ -space KKR-CPA method. For the average moments both methods show that additions of Ta to Py rapidly reduce the magnetic moment and that the magnetic moment vanishes in the neighborhood of 50% Ta. The LSMS results show that the averaging process inherent in the KKR-CPA hides significant fluctuations in the individual Fe and Ni site moments. Furthermore, for Ni sites in particular, the reductions in the site moments are larger for Ni sites that are near neighbors of Ta. Interestingly, the Ta moment is antiparallel to those of Ni and Fe. A clear explanation of the negative polarization is presented in Johnson *et al.*<sup>11</sup> for the case of  $\text{V}_x\text{Fe}_{1-x}$  alloys. In the case of  $\text{Py}_{0.9}\text{Ta}_{0.1}$  alloy, the Ni spin up and spin down  $d$ -scattering resonance energies lie

well below Ta  $d$ -scattering resonance energies. Despite the large energy difference, it is still the case that the energy separation between the Ni and Ta levels in the spin down channel is smaller than for the spin up channel. This leads to a stronger interaction between Ni and Ta in the spin down channel than in the spin up channel which in turn leads to a shift of spin down (bonding) states to lower energy and a reversal of the moment direction relative to Ni.

#### ACKNOWLEDGMENTS

The work performed at Oak Ridge National Laboratory was supported by the Office of Basic Energy Sciences, Division of Materials Science and Engineering and Office of Advanced Scientific Computing Research, Mathematics, Information and Computational Sciences Division, U.S. Department of Energy. Oak Ridge National Laboratory is operated by UT-Battelle, LLC, for the U.S. Department of Energy under Contract No. DE-AC05-00OR22725.

- <sup>1</sup>M. Kowalewski, W. H. Butler, N. Moghadam, G. M. Stocks, T. C. Schulthess, K. J. Song, J. R. Thompson, A. S. Arrott, T. Zhu, J. Drewes, R. R. Katti, M. T. McClure, and O. Escorcia, *J. Appl. Phys.* **87**, 5732 (2000).
- <sup>2</sup>H. Winter and G. M. Stocks, *Phys. Rev. B* **27**, 882 (1983).
- <sup>3</sup>B. L. Gyorffy, D. D. Johnson, F. J. Pinski, D. M. Nicholson, and G. M. Stocks, *NATO ASI Ser., Ser. E* **163**, 421 (1989).
- <sup>4</sup>Y. Wang, *Phys. Rev. Lett.* **66**, 1438 (1991).
- <sup>5</sup>G. M. Stocks, D. M. C. Nicholson, Y. Wang, W. A. Shelton, Z. Szotek, and W. M. Temmerman, in *High Performance Computing Symposium; Grand Challenges in Computer Simulation*, Proceedings of the 1994 Simulation Multiconference, edited by A. M. Tentner (The Society for Computer Simulation, San Diego, 1994).
- <sup>6</sup>J. W. Strutt and Baron Rayleigh, *Philos. Mag.* **34**, 4816 (1892).
- <sup>7</sup>W. Kohn and L. J. Sham, *Phys. Rev.* **137**, A1696 (1965).
- <sup>8</sup>P. Hohenberg and W. Kohn, *Phys. Rev.* **136**, B864 (1964).
- <sup>9</sup>G. M. Stocks, W. M. Temmerman, and B. L. Gyorffy, *Electrons in Disordered Metals and at Metallic Surfaces*, edited by P. Phariseau, B. L. Gyorffy, and L. Scheire (Plenum, London, 1978), p. 193.
- <sup>10</sup>X. G. Zhang and D. M. C. Nicholson, *Phys. Rev. B* **60**, 4551 (1999).
- <sup>11</sup>D. D. Johnson, F. J. Pinski, and J. B. Staunton, *J. Appl. Phys.* **61**, 3715 (1987).